Temperature Dependence of Molecular Line Strengths and Fe I 1565 nm Zeeman Splitting in a Sunspot

M.J. Penn
National Solar Observatory, 950 N Cherry Ave, Tucson AZ 85719 and California State University Northridge, Department of Physics and Astronomy, 18111 Nordhoff St, Northridge CA 91330-8268

S. Walton, G. Chapman, J. Ceja
San Fernando Observatory and California State University Northridge, Department of Physics and Astronomy, 18111 Nordhoff St, Northridge CA 91330-8268

W. Plick
Connecticut College, Department of Physics and Astronomy, Box 5361, 270 Mohegan Avenue, New London, CT 06320-4196

Abstract. Spectroscopic observations at 1565 nm were made in the eastern half of the main umbra of NOAA 9885 on 1 April 2002 using the National Solar Observatory McMath-Pierce Telescope at Kitt Peak with a tip-tilt image stabilization system and the California State University Northridge - National Solar Observatory infrared camera. The line depth of the OH blend at 1565.1 nm varies with the observed continuum temperature; the variation fits previous observations except that the continuum temperature is lower by 600 K. The equivalent width of the OH absorption line at 1565.2 nm shows a temperature dependence similar to previously published umbral molecular observations at 640 nm. A simple model of expected OH abundance based upon an ionization analogy to molecular dissociation is produced and agrees well with the temperature variation of the line equivalent width. A CN absorption line at 1564.6 nm shows a very different temperature dependence, likely due to complicated formation and destruction processes. Nonetheless a numerical fit of the temperature variation of the CN equivalent width is presented. Finally a comparison of the Zeeman splitting of the Fe I 1564.8 nm line with the sunspot temperature derived from the continuum intensity shows an umbra somewhat cooler for a given magnetic field strength than previous comparisions using this infrared 1564.8 nm line, but consistent with these previous infrared measurements the umbra is hotter for a given magnetic field strength than magnetic and temperature measurements at 630.2 nm would suggest. Differences between the 630.2 nm and 1564.8 nm umbral temperature and magnetic field relations is explained with the different heights of formation of the lines and continua at these wavelengths.

1. Introduction

The absorption spectra of diatomic molecules appearing in sunspots have been cataloged at visible wavelengths (Boyer, Sotirovski and Harvey, 1982) and at infrared wavelengths (Wallace, Hinkle and Livingston, 2001). The Doppler shifts of molecular spectral lines have been used to study oscillations inside sunspot umbra (Bhatnagar, Livingston, and

© 2002 *Kluwer Academic Publishers. Printed in the Netherlands.*

Harvey 1972, Penn and LaBonte, 1993). The Zeeman patterns of several molecules have been studied (Harvey, 1973) often with puzzling results until a recent formulation of molecular Zeeman splitting (Berdyugina and Solanki, 2002) has successfully explained these observations. Recent measurements of the spatial variations of the molecular line strength in sunspot umbra (Ruedi, Solanki and Livingston, 1995 and Rabin, Clark and Bergman, 2000) revealed the potential for using molecules to map the temperature in sunspots. In this work the temperature dependence of the absorption line strength of OH lines at 1565.1 and 1565.2 nm and the absorption line from CN at 1564.6 nm in and near the main umbra of NOAA 9885 is explored.

The temperature dependence of the total magnetic field strength as measured by the Zeeman splitting of the 1564.8 nm Fe I line has been published for a number of sunspots by various authors (Kopp and Rabin, 1992, Solanki, Walther and Livingston, 1993, Lin 2000, Penn *et al.* 2002, and Livingston 2002) as well as for spectropolarimetric observations of sunspots at visible wavelengths (Gurman and House, 1981, Lites *et al.* 1993, Martinez-Pillet and Vazquez, 1993, and Stanchfield, Thomas and Lites, 1997). An analysis of these published observations and new observations are presented here.

2. Observations and Reduction

The National Solar Observatory (NSO) McMath-Pierce (McM/P) telescope is described in detail by Pierce (1964) and infrared observations have been made with the main spectrograph by a number of authors. These observations used the main heliostat feeding the main spectrograph with the infrared grating. The California State University(CSUN)/NSO infrared camera is a HgCdTe based system, using a 256x256 pixel (40 micron pixel size) detector and was built by Rockwell Imaging Sciences Division in Camarillo, California. The camera gain was measured at 3 electrons per ADU with about 110 electrons read noise. The camera timing electronics are initialized with values downloaded via a RS232 serial line from the control computer, a 600 MHz Pentium-III PC system. The camera frames are read with a Data Translation DT3157 frame grabbing card and digitized for use in the PC; control software written in Research System Inc. Interactive Data Language (IDL) communicates with the DT3157 via Dynamically Linked Library code. The frames are written to a local hard disk in a FITS format; maximum frame rate achieved is about 17 frames per second. A polarimeter system was tested during these observations and was completed in 2002; it will be discussed in future work.

Reimaging optics at the spectrograph exit port provided a spatial scale of 0.6 arcseconds per pixel and a spectral scale of of 7.3 pm (73 milli-Å) per pixel on each spectral frame. Telescope scanning for much of the observing run was done by manually controlling the main heliostat pointing. However for this run the new McM/P adaptive optics system was used to stabilize the image by making tip-tilt corrections only. The AO system allowed a small field-of-view to be scanned while tip-tilt correction was active, and so the eastern half of the main umbra of NOAA 9885 was scanned in this mode. The step size perpendicular to the slit was about 0.25 arcseconds, although this oversampled the poor seeing present during the observations.

3. Discussion

The images were dark subtracted in the usual way, and a spectral flat field image was taken at the same wavelength in focus and processed using an algorithm similar to Jones (1999). Figure 1 shows sample spectra from one spatial pixel each in the photosphere and the sunspot umbra, and Figure 2 shows a sample spectral frame from which the continuum variations have been removed by subtracting the intensity values at 1565.5 nm (averaged over about 0.1 nm) from each column of the image. In this Figure the molecular lines and Zeeman splitting are visible in the umbral spectra and not in the photospheric spectra.

The field-of-view of the observations on the solar surface is shown in Figure 3. Maps of the continuum intensity, the OH 1565.2 nm line strength, the CN 1564.6 nm line strength, and the Zeeman spitting of the Fe I 1564.8 nm line are shown in each subwindow. Each subframe measures roughly 150 arcseconds in the north-south direction and 25 arcseconds in the east-west direction; the spectrograph slit was oriented in the north-south direction, and the image was scanned in the east-west direction using a manual control of the new McM/P AO system. While the tip-tilt correction removed image motion, significant image blur can be seen in Figure 3 due to the rather poor seeing present during the observations.

The temperature in NOAA 9885 was computed from the ratio of the continuum intensity to the photospheric continuum intensity taken from the nearby solar photosphere, assuming the continuum is described by the Planck function. At a spatial pixel the intensity ratio R is measured, and the temperature is computed using:

$$T = \frac{hc/k\lambda}{ln((e^{hc/k\lambda T_{photo}} - 1)/R + 1)}$$

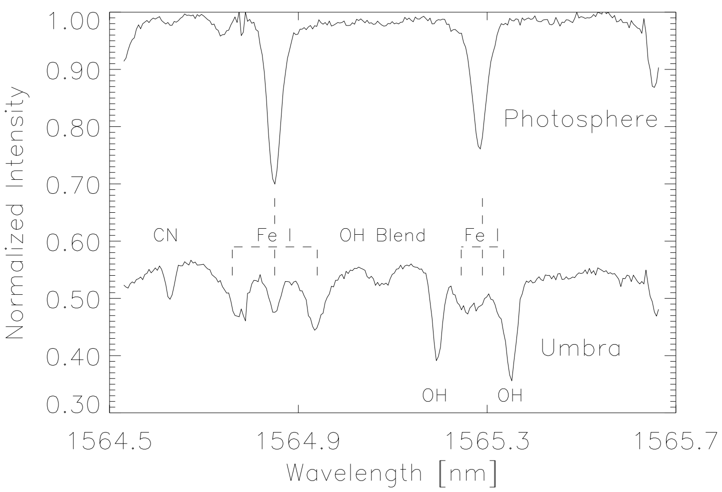

Figure 1. A sample photospheric spectrum from 37 arcseconds spatial position and an umbral spectrum from spatial position 72 arcseconds in the western-most spectral frame (shown in Figure 2). In addition to the labeled spectral lines, three additional Fe I lines can be seen: a weak line at 1564.75 nm, and two lines at either edge at 1564.5 and 1565.7 nm. In the umbral spectrum both strong Fe I lines show Zeeman splitting and the tick marks represent splitting from a 2600 Gauss magnetic field.

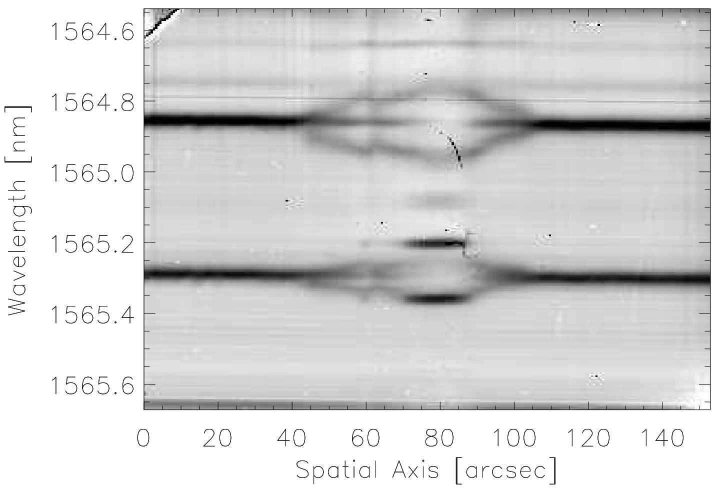

Figure 2. The western-most spectral frame from the scan of the sunspot umbra of NOAA 9885. Each spectrum in this frame (each column in the image) has the continuum removed by simply subtracting the averaged intensity at 1565.6 nm. By removing the large intensity variations due to the sunspot penumbra and umbra, the Zeeman splitting in the Fe I lines and the appearance of the molecular lines are enhanced. Also visible near the frame center are several flat-fielding artifacts.

Figure 3. Images of the eastern half of the umbra of NOAA 9885 taken at the McMath-Pierce telescope with the CSUN-NSO IR camera. The four subframes show (left to right): the continuum variation at 1565.5 nm, the 1565.3 nm OH line strength, the 1564.6 nm CN line strength, and the splitting of the Zeeman components of the g=3 Fe I 1564.85 nm line. The apparent weakening of the CN line strength in the umbral center is real and discussed in the text. In each subframe geocentric north is up and east is left.

where T_{photo} is the photospheric temperature taken from Vernazza, Avrett and Loeser (1976); $T_{photo} = 6000$ K at 640 nm $T_{photo} = 6640$ K at 1565 nm.

3.1. OH Line Strength Variations

The normalized line depth measured from the 1565.1 nm OH line compares favorably to the fit from Rüedi *et al.* (1995) (see Figure 4) with the exception that the temperature in the polynomial from Rüedi *et al.* (1995) is replaced with $T+600$ K in these observations. It is possible that since their work involved a sunspot with a prominent light bridge and NOAA 9885 showed no such feature, the Rüedi *et al.* . temperatures are systematically higher because of continuum radiation from the light bridge; or differences between the model continuum temperatures used in that work and the simple temperature calculation made in this work may explain the difference. While the 1565.1 nm line is spectrally well-separated from the Fe I lines, it is a blend of two OH absorption features and is a relatively weak spectral feature.

The OH lines at 1565.2 and 1565.3 nm are much stronger absorption features, but they are located spectrally close to the Fe I 1565.3 nm

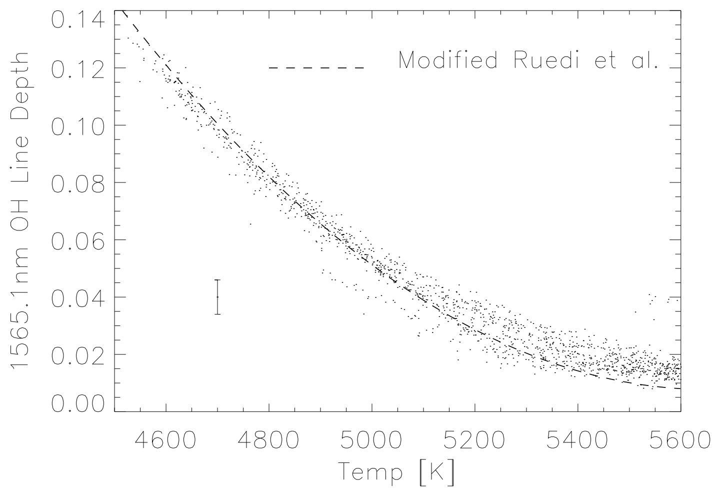

Figure 4. Line depth values for the OH blend at 1565.1 nm for NOAA 9885 are similar to the results from Ruedi *et al.* (1995) except that the temperature must be reduced by 600 K. Shown are the computed equivalent widths versus continuum temperature and the polynomial fit from Ruedi *et al.* (1995) computed at a temperature T + 600 K. The point in the lower left shows the estimated 3 σ measurement errors.

line. When this Fe I line Zeeman splits in a sunspot umbra there is some contamination of the OH lines. However, the temperature dependence of the equivalent width measured from the 1565.2 nm OH line in NOAA 9885 roughly agrees with measurements from a TiO/CN umbral molecular line at visible wavelengths made in 1991 of NOAA 6619 (Penn and LaBonte, 1993). The TiO/CN equivalent width has been arbitrarily multiplied by a factor of 7.5 to account for inherent line strength differences between the two spectral lines, and the equivalent widths of both lines are plotted in Figure 5. Equivalent width measurements from an OH absorption line at 1645 nm from Wallace, Hinkel and Livingston (2001) are also plotted in Figure 5, again arbitrarily scaled to match the 1565.2 nm OH line widths to account for inherent differences in the line strengths. While these different molecular lines are not expected to behave identically with changing temperatures, the fact that the 1565.2 nm OH line shows the same temperature dependence to within about 5 mÅ of equivalent width means that contamination from the Zeeman-split component of the Fe I 1565.3 nm line is not very large in these measurements. For sunspots with different (larger) Zeeman splitting the contamination may be larger.

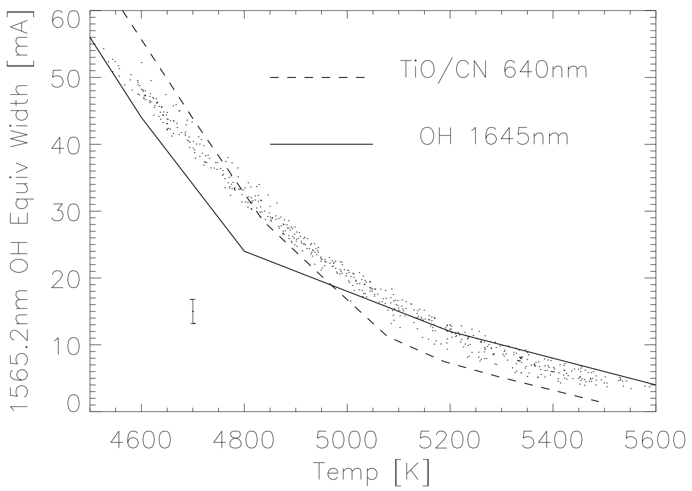

Figure 5. The measured equivalent width of the 1565.3 nm OH line shows a temperature dependence similar to measurements of a TiO/CN blend (Penn and LaBonte, 1993) and the 1645 nm OH absorption line (Wallace, Hinkle and Livingston, 2001). In both cases the previous measurements are arbitrarily scaled to best fit the 1565.3 nm data simply reflecting the difference in inherent line strengths. No shift in the temperature is made. The point in the lower left shows the estimated 3 σ measurement errors.

Certainly there is no physical reason to believe that the line depth versus temperature will behave as a polynomial; how should the line strength vary with temperature? For a physical model of the expected temperature behavior of the molecular line strength it is instructive to examine simple molecular abundance models even without a complete treatment of the level populations or the radiative transfer. With the assumptions of local thermodynamic equilibrium and an optically thin umbral molecular atmosphere the absorption strength of the OH line is expected to follow the column density of OH absorbers. The number of OH absorbers present will be proportional to the lifetime of the OH molecule, which should be inversely related to the destruction rate of OH. Among the many physical and chemical destruction processes are collisional and radiative dissociation of the molecule. A simple model of collisional and radiative dissociation can be drawn from collisional and radiative ionization models, and in the following discussion it is assumed that the temperature dependence of the dissociation processes are identical to the ionization processes. Collisional ionization as discussed in Mihalas (1978) makes simplifying assumptions that the particle velocity distribution is Maxwellian and that the collisional cross-section is equal to the semi-classical Thomson scattering cross-section. With these assumptions a model of the collisional dissociation rate $C_{i\kappa}$ based on ionization has a temperature dependence of $C_{i\kappa} \sim T^{1/2}e^{-h\nu_D/kT}$ where $h\nu_D$ is the dissociation energy of the $X^2\Pi$ state equal to 4.2 eV (Van Dishoeck and Dalgarno, 1984) rather than the ionization energy. Similarly the temperature dependence of the radiative dissociation rate $R_{i\kappa}$ can be shown to vary as $R_{i\kappa} \sim Te^{-h\nu_D/kT}$ where again $h\nu_D$ is the dissociation energy.

If the equivalent width of the molecular lines W is directly proportional to the lifetime of the molecules, the reciprocals of the collisional and radiative rates can be used to predict the equivalent width. The equivalent widths $W_r \sim 1/R_{i\kappa}$ and $W_c \sim 1/C_{i\kappa}$ are computed and are normalized to the measured OH equivalent widths near $T = 5000$K where the equivalent width is roughly 20 mÅ, and the OH measured equivalent widths and the collisional and radiative predicitive curves are shown in Figure 6. Although both curves deviate from the measured equivalent widths, the models can correctly explain almost a factor of five change in the molecular line equivalent width within the measurement scatter. An analysis of the measured line width and line depth suggest that saturation effects may slightly influence the OH line at the largest equivalent widths, and this may explain some of the deviations from the models at low temperatures. The discrepancy at higher temperatures is more difficult to explain and may be an effect of stray light. But ignoring these deviations there are two conclusions that can be drawn from the relative success of this model; first the photospheric umbral temperature measured with the continuum intensity is closely related to the plasma temperature at the height of formation of the OH line, and second the molecular OH abundance in the plasma is the most important factor in determining the variation of the absorption line strength.

With the normalization constant involved in the comparison of the data with the dissociation models, the absolute temperature measurements from this data cannot be verified. A determination of the absolute temperature using only one molecular line is difficult; the measurement can be done by measuring several line strengths preferably from lines with large energy differences and using a population diagram analysis (Goldsmith and Langer, 1999). However the confidence in the relative temperature changes observed across the field-of-view is strengthened by the measured OH line strength.

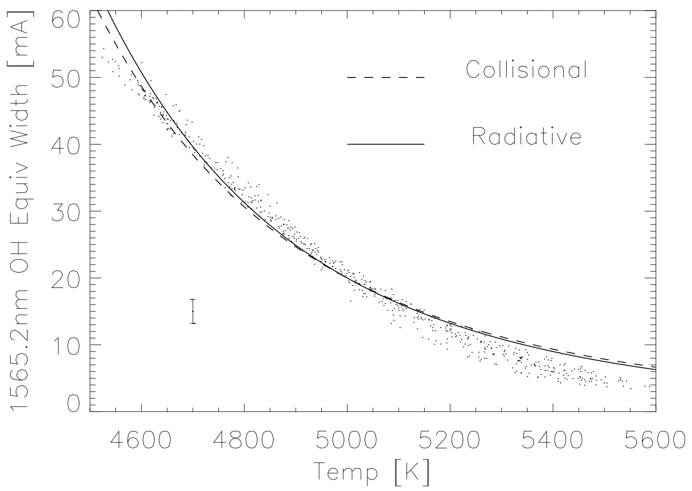

Figure 6. Simple collisional and radiative dissociation models predict a temperature dependence of the OH line equivalent width very similar to the observations. Each model is arbitrarily normalized to the observed equivalent width at T = 5000 K to account for the inherent line strength; deviations at high and low equivalent widths likely reflect the simplistic assumptions in these models and call for more complete physical descriptions. The point in the lower left shows the estimated 3 σ measurement errors.

3.2. CN Equivalent Width Variations

The temperature dependence of the 1564.6 nm CN molecular absorption line equivalent width is different from the widths of the OH lines. The CN equivalent width shows a peak at about 4900K as shown in Figure 7; at lower temperatures in the umbra the line becomes weaker as seen in Figure 3. The same peak is seen in the 1164 nm CN line equivalent width in the work of Wallace, Hinkle and Livingston (2001) and an interpolation of their measurements is shown in Figure 7. Both of these results agree with the observed umbral behavior of other CN lines (Harvey, 1973).

In order to fit the CN equivalent width a function $W(T)$ is used with the general form $W(T) \sim aT^x e^{mT_D/T}$ where a is a constant, T is the temperature, T_D is the dissociation temperature, $m = \pm 1$, and x is positive or negative. The existance of a peak in the equivalent width helps to eliminate possible values of both x and m. Functions where x and m have opposite signs have first derivatives equal to zero only for negative values of temperature T and these are unphysical solutions. Functions where both x and m are positive have only a local minimum at positive temperature, and so only functions where both x

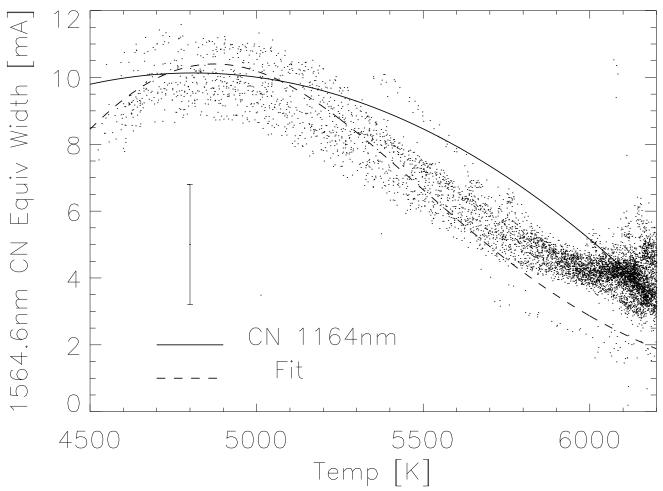

Figure 7. The measured equivalent width of the CN 1564.8 nm line in NOAA 9885 compared with the equivalent width of 1164 nm CN absorption as reported by Wallace, Hinkle and Livingston (2001). The fit to the equivalent width is numerically convenient but likely does not have much physical relevence (see text). The point in the lower left shows the estimated 3 σ measurement errors.

and m are negative have a local maximum at a positive temperature. The position of this maximum defines the ratio of x/T_D. Finally the constant a and the values of x and T_D are determined with two points from the data; the resulting function $W(T) = e^{607.8} T^{-63.8} e^{-310900/T}$ is also shown in Figure 7. While this mathematical function does a good job of fitting the temperature dependence of the CN equivalent width, it is unlikely to explain the underlying physics behind the formation of the molecule for two reasons. First, the extremely steep temperature dependence contradicts both the simple collisional and radiative dissociation models discussed above as well as studies of the CN chemistry where the production and destruction rates of CN were only weakly dependent upon temperature (Hollenbach and McKee, 1979, Federman *et al.* 1994). Secondly the dissociation temperature value $T_D = 310900$ implies a dissociation energy $h\nu_D = kT_D = 26.8$ eV much higher than that reported for the $X^2\Sigma^+$ state of CN of $h\nu_D = 7.77$ eV (Costes, Naulin and Dorthe 1990). Although the CN equivalent width does vary dramatically with plasma temperature, it would seem that processes more complicated than this simple dissociation model are dominating the CN equivalent width. Any procedure aimed at deriving the plasma temperature from the CN line strength must include the chemical reactions involved in the CN equilibrium.

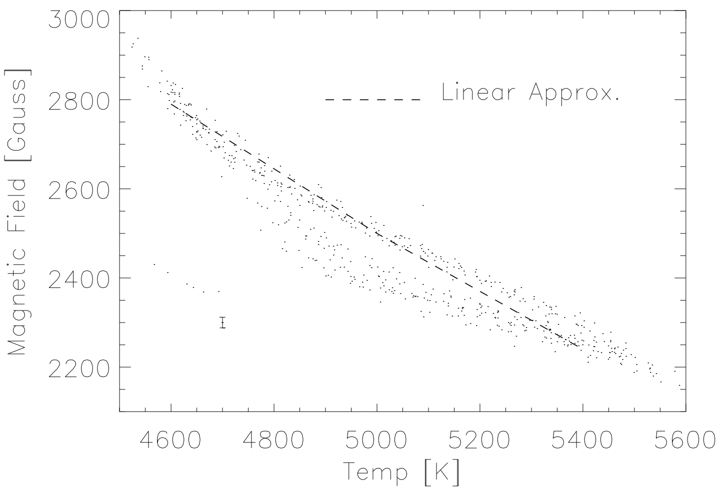

Figure 8. The measured magnetic field strength versus continuum temperature in NOAA 9885. Systematic flat fielding errors are likely the cause of the apparent gap at temperatures near 5000 K. The line shows a linear approximation made to the data which appears as the "Penn2" line in Figure 9. The point in the lower left shows the estimated 3 σ measurement errors.

4. Zeeman Splitting and Temperature

The Zeeman components of the Fe I 1564.8 nm line were fit with Gaussian functions and the distance between the two components was measured in the umbral pixels and through most of the penumbral pixels. A plot of the magnetic field strength determined from this splitting compared to the temperature from the continuum intensity at each pixel is shown in Figure 8, and a linear approximation to these measurements is also shown. As in many previous studies, the temperature dependence of the magnetic splitting is not a simple linear function. Of particular interest is the steep dependence of the magnetic field with temperature at the lowest temperatures, a common feature in many other measurements and explored in depth by Lin (2002). The scatter in these measurements is less than that seen by other authors, perhaps due to smoothing caused by the poor seeing conditions.

Observations from the several infrared and optical studies referenced in the Introduction are shown in Figure 9. Included are measurements of only the darkest regions of many sunspots over two solar cycles by Livingston (2002). Each plot is a very simple linear interpretation of the locus of points shown by each author; there is non-linear dependence and significant scatter in the original measurements around the simple

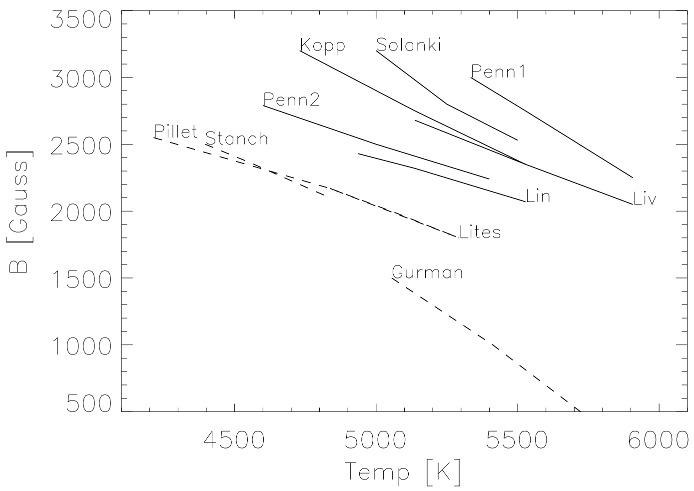

Figure 9. The magnetic field strength versus temperature relationship for several authors. Measurements using the 630.2 nm line are dashed, and observations using the near-infrared 1564.8 nm line are solid lines. Only a simple linear approximation was made to the published data; a large scatter and non-linear behavior may be present in the original measurements. Accounting for temperature and magnetic vertical gradients associated with the two wavelengths would shift the "Lites" line to the exact position of the "Liv" results.

lines plotted in Figure 9. These deviations can be estimated by the example in Figure 8, however the reader is referred to the original papers for further details. Two items of interest are revealed by Figure 9. First, there is a systematic difference between the visible and the infrared observations. The visible observations are located either 1000K cooler or at 1200 Gauss lower magnetic field than extrapolation of the infrared observations might suggest. Even the earliest work at 630 nm by Gurman (1981) extrapolates correctly to the more recent 630 nm measurements and misses the region occupied by the infrared measurements.

Bruls *et al.* (1991) compute umbral heights of formation of 190 km and 19 km for the 630.n nm and 1564.8 nm lines respectively. Using the 170 km height difference, a systematic reduction in the magnetic field strength of 1200 Gauss would imply a vertical gradient $\delta B/\delta h$ of 7 Gauss km^{-1}, signficantly higher than that measured by Pahlke and Wiehr (1990) of 2 Gauss km^{-1} in a sunspot umbra using several lines near 615 nm, and higher than the 2 Gauss km^{-1} gradient measured at the inner penumbral boundary by Moran *et al.* (2000) using the 1564.8 nm line and the 12320 nm Mg I line. Using these measured vertical gradients imply that the 630.2 nm magnetic fields would need to be increased by 340 Gauss to compare with the 1564.8 nm measurements.

The temperature difference at the heights of formation of the continuum at these two wavelengths can be estimated by using heights of -26 km and 13 km for the 1564.8 nm and 630.2 nm continua (Vernazza, Avrett and Loeser, 1976) and then using atmospheric models of sunspots to compute a temperature difference. Using the M4 model of Kollatschny *et al.* (1980) these heights imply a temperature difference of 470 K, while usign the umbral model of Collados *et al.* (1994) implies an expected temperature difference of 590 K. Using these values for $\delta T/\delta h$ suggests adding about 500 K to the temperatures of the 630.2 nm in order to compare with the infrared measurements. When 340 Gauss and 500 K are added to the results from Lites *et al.* (1993) the linear approximation moves to exactly the position of the Livingston (2002) linear approximation. The difference between the visible and infrared measurements can be exactly accounted for by adjusting for the height variations of temperature and magnetic field expected for these two different wavelengths.

The second feature of Figure 9 is the significant scatter in results from the infrared measurements, even from measurements using the same telescope and spectrograph show large differences (as comparing the lines "Penn2" and "Kopp" shows). It is interesting to speculate about how much of the differences observed truly represent real physical differences between sunspots. Long-term observations of this type, with associated instrumental scattered light measurements, will provide an interesting look at differences between sunspots, and would address the solar-cycle related changes seen by Livingston (2002).

5. Acknowledgements

Thanks go to C. Plymate and E. Galayda for immeasureable help at the telescope during the observations, and C. Keller for help with the new AO system. The CSUN-NSO camera was purchased using the AFOSR award F49620-00-1-0355. J. Ceja was supported with NSF grant ATM-0077624, and W. Plick was supported by the 2002 NSO NSF-REU program. MJP would like to thank J. Harvey for a thorough reading and several comments on this manuscript.

References

Berdyugina, S.V., and Solanki, S.K. : 2002, *Astron. Astrophys.* **385,** 701.

Bhatnagar, A., Livingston, W.C., and Harvey, J.W. : 1972, *Solar Phys.* **27** 80.

Boyer, R., Sotirovski, P., and Harvey, J.W. : 1982, *Astron. Astrophys. Suppl. Ser.* **47,** 145.

Bruls, J.H.M.J., Lites, B.W., and Murphy, G.A. : 1991, in *Solar Polarimetry, Proceedings of the Eleventh NSO/Sac Peak Workshop*, ed. L.J. November (NSO: Sunspot), 444

Collados, M., Martinez Pillet, V., Ruiz Cobo, B., del Toro Iniesta, J.C., and Vazquez, M. : 1994, *Astron. Astrophys.* **291,** 622.

Costes, M., Naulin, C., and Dorthe, G. : 1990, *Astron. Astrophys.* **232,** 270.

Federman, S.R., Strom, C.J., Lambert, D.L., Cardelli, J.A., Smith, V.V. and Joseph, C.L. : 1994, *Astrophys. J.* **424**, 772.

Goldsmith, P.F. and Langer, W.D. : 1999, *Astrophys. J.* **517**, 209.

Gurman, J.B. and House, L.L. : 1981, *Solar Phys.* **71** 5.

Harvey, J.W. : 1973, *Solar Phys.* **28** 43.

Hollenbach, D., and McKee, C.F. : 1979, *Astrophys. J. Suppl Ser* **41**, 555.

Jones, H.P. : 1999, *BAAS* **31**, 958.

Kollatschny, W., Stellmacher, G., Wiehr, E., and Falipou, M.A. : 1980, *Astron. Astrophys.* **86,** 245.

Kopp, G. and Rabin, D. : 1992, *Solar Phys.* **141** 253.

Lin, H. : 2002, *BAAS* **34**, 690.

Lites, B.W., Elmore, D.F., Seagraves, P. and Skumanich, A.P. : 1993, *Astrophys. J.* **418**, 928.

Livingston, W. : 2002, *Solar Phys.* **207** 41.

Martinez Pillet, V. and Vazquez, M. : 1993, *Astron. Astrophys.* **270,** 494.

Mihalas, D. : 1978, in *Stellar Atmospheres*, W. H. Freeman, New York.

Moran, T., Deming, D., Jennings, D.E., and McCabe, G. : 2000, *Astrophys. J.* **533**, 1035.

Pahlke, K.D., Wiehr, E. : 1990, *Astron. Astrophys.* **228,** 246.

Pierce, A.K. : 1964, *Applied Optics* **3**, 1337.

Penn, M.J. and LaBonte, B.J. : 1993, *Astrophys. J.* **415**, 383.

Penn, M.J., Ceja, J.A., Bell, E., Frye, G. and Linck, R. : 2002, *Solar Phys.* **205** 53.

Rabin, D., Clark, T.A., and Bergman, M.W. : 2000, *BAAS* **32**, 804.

Rüedi, I., Solanki, S.K. and Livingston, W. : 1995, *Astron. Astrophys.* **302,** 543.

Solanki, S.K., Walther, U. and Livingston, W. : 1993, *Astron. Astrophys.* **277,** 639.

Stanchfield II, D.C.H., Thomas, J.H. and Lites, B.W. : 1997, *Astrophys. J.* **477**, 485.

Van Dishoeck, E.F. and Dalgarno, A. : 1984, *Icarus* **59** 305.

Vernazza, J.E., Avrett, E.H. and Loeser, R. : 1976, *Astrophys. J. Suppl Ser* **30**, 1.

Wallace, L., Hinkle, K., and Livingston, W. : 2001, "Sunspot Umbral Spectra in the Region 4000 to 8640 cm^{-1} (1.16 to 2.50 μm)" N.S.O. Technical Report #01-001, Tucson, AZ.